



PERGAMON

International Journal of Heat and Mass Transfer 44 (2001) 2475–2481

International Journal of  
**HEAT and MASS  
TRANSFER**

www.elsevier.com/locate/ijhmt

# Study on film boiling heat transfer for water jet impinging on high temperature flat plate

Zhen-Hua Liu <sup>\*</sup>, Jing Wang

*School of Power and Energy Engineering, Shanghai Jiaotong University, Shanghai 200030, People's Republic of China*

Received 21 March 2000; received in revised form 28 August 2000

## Abstract

An theoretical and experimental study on film boiling heat transfer for water jet impinging on the horizontal high temperature flat plate is performed for the jet stagnation zone. Simplified two-phase flow boundary layer equations were used to calculate the thickness of the vapor layer and from it the heat transfer coefficient of film boiling is obtained. A semi-empirical correlation is proposed for predicting the heat transfer coefficient of film boiling. © 2001 Elsevier Science Ltd. All rights reserved.

*Keywords:* Film boiling; Two-phase flow; Water jet impinging cooling; Stagnation heat transfer

## 1. Introduction

Water jet impinging cooling of hot plate, as a high effective cooling method, has been widely used in iron and steel industry, nucleate power process and some microelectronic devices making and thermal management process. According to the range of plate temperatures, the heat transfer statuses may be divided into forced convection, nucleate boiling, transitive boiling and film boiling. Especially, it is very important for understanding the heat transfer characteristics of film boiling or transitive boiling for actual cooling process of strip mills and emergent cooling of nucleate power devices.

For forced convective heat transfer of water jet, various theoretical and experimental studies have been reported in open literatures [1–5]. Miyazaki and Siberman [6] and Watson and Viskanta [7] carried out numerical studies on velocity distributions and forced convective heat transfer characteristics.

For nucleate boiling of water jet, many experimental investigations have been conducted to understand the heat transfer characteristics of water jet flow [8,9]. Kumagai et al. [10] investigated experimentally transi-

tive boiling heat transfer characteristics of the two-dimensional water jet flow.

Only a few of works have been reported for film boiling of water jet. Ishitani et al. [11] carried out a numerical and experimental study for film boiling heat transfer of two-dimensional water jet. Zumbrennen et al. [12] investigated experimentally the film boiling heat transfer characteristics for an actual strip mill. Zhe et al. [13] investigated experimentally the boiling heat transfer characteristics for water jet in the whole boiling regions. Theoretical and experimental studies are still needed. It is insufficient and even inconsistent to understand the effects of various parameters on the heat transfer. For a round or two-dimensional water jet impinging on a flat plate, the governing parameters of film boiling mainly includes the heat flux or the superheating of wall, jet diameter or jet width, jet velocity and the subcooling of water. The subcooling of water is important for the heat transfer status and the heat transfer coefficient in high temperature range.

In this paper, a theoretical analysis and experimental investigation on film boiling heat transfer of water jet impinging on high temperature flat plate is performed for the jet stagnation zone. A theoretical model of two-phase flow boundary layers is applied to analyze the thickness of boundary layer of vapor and water. A semi-empirical correlation is suggested finally for the stagnation heat transfer of water impinging jet cooling.

<sup>\*</sup> Corresponding author. Fax: +86-21-62932280.

*E-mail address:* liuzhenh@guomai.sh.cn (Z.-H. Liu).

Nomenclature			
$c_p$	Specific heat of test specimen ( $\text{J kg}^{-1} \text{K}^{-1}$ )	$\lambda$	Thermal conductivity ( $\text{J m}^{-1} \text{K}^{-1} \text{s}^{-1}$ )
$d$	Diameter of nozzle (m)	$\mu$	Viscosity (Pa s)
$h_{fg}$	Latent heat of evaporation ( $\text{J kg}^{-1}$ )	$\tau$	Interface stress (Pa)
$Nu$	Nusselt number	$\nu$	Kinematics viscosity ( $\text{m}^2 \text{s}^{-1}$ )
$P$	Pressure (Pa)	$\rho$	Density ( $\text{kg m}^{-3}$ )
$Pr$	Prandtl number	<i>Subscripts</i>	
$q$	Heat flux ( $\text{J m}^{-2} \text{s}^{-1}$ )	a	Atmospheric
$Re$	Reynolds number	0	Initial position at the outlet of nozzle
$r$	Distance of the radial direction (m)	r	Radiation
$T$	Temperature (K)	l	Liquid
$t$	Time (s)	s	Saturated
$u$	Velocity of the radial direction ( $\text{m s}^{-1}$ )	t	Temperature
$V$	Velocity of the vertical direction ( $\text{m s}^{-1}$ )	v	Vapor
<i>Greek symbols</i>		w	Wall
$\alpha$	Heat transfer coefficient ( $\text{J m}^{-2} \text{K}^{-1} \text{s}^{-1}$ )	$\delta$	Interface of vapor–liquid
$\delta$	Thickness of boundary layer (m)	$\infty$	The mainstream zone of liquid flow

## 2. Simplified theoretical analysis

Fig. 1(a) shows the schematic diagram of the analytical model and Fig. 1(b) shows the schematic diagram of the boundary layer of vapor and liquid and coordinate. Here, a round water jet of diameter,  $d$ , impinged vertically on a circular flat plate, with the initial jet velocity,  $V_0$ , and the initial water temperature,  $T_0$ , at the outlet of nozzle. For film boiling on high temperature flat plate, the heated surface can be divided into center jet stagnation zone and surrounding mist cooling zone. In this study, only the jet stagnation zone is considered as the object with the analytical zone as:  $0 \leq r \leq d/2$ . Evaporated vapor forms very thin vapor layer on the heated surface and the interface of vapor–liquid is assumed smooth and no waviness. As the thickness of vapor layer is so thin that the inertia force and the pressure differences in the vertical direction can

be neglected, while the temperature distribution is linear in the vapor layer. We assumed here that no coupling relation exists between the radiative and the convective heat transfer, such that the radiative heat transfer can be calculated independently as Bromley's treatment [14].

The wall heat flux supplies the evaporation heat flux of liquid, the convection heat flux of subcooled liquid and the radiative heat flux in the vapor layer, that is,

$$q_w = q_v + q_l + 3q_r/4. \quad (1)$$

At the interface of velocity boundary layer of liquid and in the mainstream zone of liquid flow, the radial velocity of liquid can be described as

$$u_{l\infty}/V_s = r/d. \quad (2)$$

Here,  $V_s$  denotes the impinging velocity at the center of the stagnation zone and is equal to the initial velocity at the outlet of nozzle,  $V_0$ , if the effect of gravity force is neglected.

At the vapor–liquid interface, i.e.,  $y = \delta_v$ , the distribution of pressure and the radial velocity can be, respectively, expressed as:

$$\frac{P - P_a}{P_s - P_a} = 1 - \left(\frac{2r}{d}\right)^2, \quad (3)$$

$$u_{\delta}/V_s = 2r/d, \quad (4)$$

where  $P_s$  denotes the stagnation pressure at the center of the stagnation zone, i.e.,  $P_s = (1/2)\rho_l V_s^2 + P_a$ .

Inside the velocity and the thermal boundary layer of liquid, the distributions of velocity and temperature are

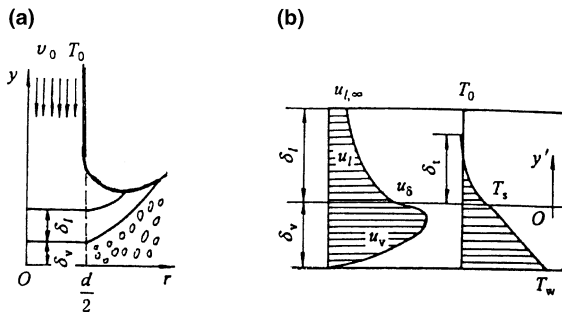


Fig. 1. Schematic diagrams of the physical model and coordinate: (a) analytical zone; (b) boundary layer of vapor and liquid at the stagnation zone, i.e.,  $0 \leq r \leq d/2$ .

taken as exponential forms along the plate surface (refer to Eqs. (2), (4) and Fig. 2), as

$$\frac{u_l - u_{l\infty}}{u_\delta - u_{l\infty}} = 1 - \frac{3}{2} \left( \frac{y'}{\delta_l} \right) + \frac{1}{2} \left( \frac{y'}{\delta_l} \right)^3, \quad (5)$$

$$\frac{T_l - T_0}{T_s - T_0} = 1 - \frac{3}{2} \left( \frac{y'}{\delta_t} \right) + \frac{1}{2} \left( \frac{y'}{\delta_t} \right)^3. \quad (6)$$

Here,  $\delta_l$  and  $\delta_t$  denote the thickness of the velocity boundary and the thermal boundary layer of liquid, respectively.  $T_s$  and  $T_0$  denote saturated temperature at the vapor–liquid interface and the mainstream temperature of liquid. We take, as usual,

$$\delta_t = \delta_l Pr_1^{-1/3}. \quad (7)$$

Inside the vapor layer, the momentum equation is simplified as

$$\mu_v \frac{\partial^2 u_v}{\partial y^2} = \frac{\partial P}{\partial r}. \quad (8)$$

Integrating Eq. (8) twice, and inducing Eqs. (3) and (4) as the boundary conditions, we have

$$u_v = \frac{2rV_s^2 \rho_l}{\mu_v d^2} (y\delta_v - y^2) + \frac{2rV_s}{d} \left( \frac{y}{\delta_v} \right). \quad (9)$$

At the vapor–liquid interface,  $y = \delta_v$ , the interfacial stress is

$$\tau_\delta = \mu_v \frac{\partial u_v}{\partial y} = \mu_l \frac{\partial u_l}{\partial y}. \quad (10)$$

Substituting Eqs. (5) and (9) into Eq. (10), and defining  $Re_l = V_s d / \nu_l$ , we have,

$$\delta_l = \frac{3}{4} \left( \frac{\mu_l}{\mu_v} \right) \delta_v \left/ \left[ Re_l \left( \frac{\mu_l}{\mu_v} \right) \left( \frac{\delta_v}{d} \right)^2 - 1 \right] \right. \quad (11)$$

At any section of the radial direction in the vapor layer, the mass conservation equation of vapor can be described as

$$2\pi r \rho_v \int_0^{\delta_v} u_v dy = \pi r^2 q_v / h_{fg}. \quad (12)$$

Bring Eq. (9) into Eq. (12), we get

$$\frac{q_v}{2h_{fg} \rho_v V_s} = \frac{Re_l}{3} \left( \frac{\mu_l}{\mu_v} \right) \left( \frac{\delta_v}{d} \right)^3 + \left( \frac{\delta_v}{d} \right). \quad (13)$$

At the vapor–liquid interface, the convective heat flux through the thermal boundary layer of subcooled liquid would be

$$q_l = -\lambda_l \left. \frac{\partial T_l}{\partial y} \right|_{y=0}. \quad (14)$$

Bring Eqs. (6) and (7) into Eq. (14), we have

$$q_l = \frac{3}{2} \lambda_l \Delta T_{\text{sub}} Pr_1^{1/3} / \delta_l. \quad (15)$$

Both  $q_l$  and  $q_v$  pass entirely the vapor layer reaching to the vapor–liquid interface, hence, according to the energy conservation,

$$q_l + q_v = \Delta T_{\text{sat}} \lambda_v / \delta_v. \quad (16)$$

1. Test specimen
2. Thin copper slat for leading electric current
3. Slide shutter
4. Jet nozzle
5. Fire proof brick
6. Rock wool Plate
7. C.A. T.C.
8. Cold junction
9. Digital recorder
10. Digital voltmeter
11. Head tank

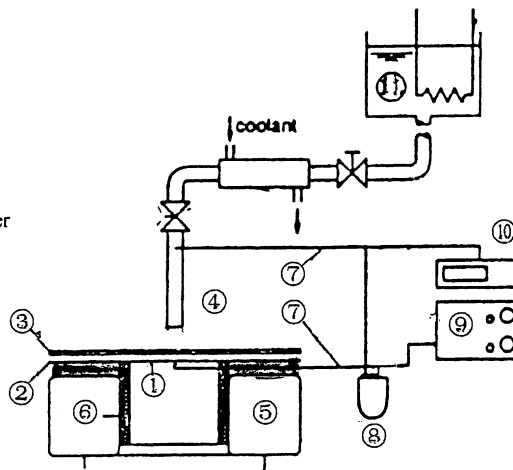


Fig. 2. Schematic diagram of the experimental setup.

Eqs. (11), (13), (15) and (16) have constructed a closed system of equations to solve  $\delta_v$ ,  $\delta_1$ ,  $q_1$  and  $q_v$  for known  $\Delta T_{\text{sat}}$ . Therefore, analytical solutions of film boiling heat transfer can be obtained. As  $\Delta T_{\text{sub}} = (T_s - T_0)$  denotes the liquid subcooling, while  $\Delta T_{\text{sat}} = (T_w - T_s)$  denotes the wall superheating, if taking  $\delta_v$  as known variable instead  $\Delta T_{\text{sat}}$ , then  $\delta_1$ ,  $q_1$ ,  $q_v$  and  $\Delta T_{\text{sat}}$ , corresponding to  $\delta_v$ , can be easily evaluated. The film boiling curves of  $q_w$  against  $\Delta T_{\text{sat}}$  may thence be plotted. According to trial calculations, the range of  $\delta_v$  is about 20–100  $\mu\text{m}$ .

Generally,  $(\delta_v/d)$  is very small and  $Re_1(\mu_l/\mu_v)$  is greater at least one order of magnitude than  $(\delta_v/d)^2$ . Hence, Eqs. (11) and (13) may be simplified as

$$\delta_1 = \frac{3}{4} \frac{d^2}{Re_1 \delta_v}, \quad (17)$$

$$\frac{q_v}{h_{\text{fg}} \rho_v V_s} = \frac{2}{3} \left( \frac{\delta_v}{d} \right)^3 \left( \frac{\mu_l}{\mu_v} \right) Re_1. \quad (18)$$

From Eqs. (17) and (18), the wall temperature and the wall heat flux will be uniform in the stagnation zone.

For saturated liquid,  $\Delta T_{\text{sub}} = 0$ ,  $q_1 = 0$  in Eq. (16), and thereby  $q_w = q_v + 3q_r/4$ , bring Eq. (18) into Eq. (1), we get

$$q_w = \left( \frac{\Delta T_{\text{sat}} \lambda_v}{d} \right)^{3/4} \left( \frac{2}{3} h_{\text{fg}} V_s Re_1 \mu_l / v_v \right)^{1/4} + \frac{3}{4} q_r. \quad (19)$$

For the case in which liquid bring high subcooling,  $q_1$  is much larger than  $q_v$  and  $q_r$  ( $q_r < 10^4 \text{ W m}^{-2}$ ), hence,  $q_v$  and  $q_r$  may be even neglected. Combining Eqs. (16), (17) and Eq. (15), we have

$$q_w \approx q_1 = 1.414 Re_1^{1/2} Pr_1^{1/6} (\lambda_l \lambda_v \Delta T_{\text{sub}} \Delta T_{\text{sat}})^{1/2} / d. \quad (20)$$

For the two-dimensional jet impinging flow, the above-mentioned analysis process is still available, except removing the factor 2, on the left-hand side of Eq. (12). Then, for saturated liquid,  $\Delta T_{\text{sub}} = 0$ ,

$$q_w = \left( \frac{\Delta T_{\text{sat}} \lambda_v}{d} \right)^{3/4} \left( \frac{1}{3} h_{\text{fg}} V_s Re_1 \mu_l / v_v \right)^{1/4} + \frac{3}{4} q_r, \quad (21)$$

where  $d$  denotes the width of jet flow. For highly subcooled liquid, Eq. (20) can also be available for two-dimensional jet flow.

With Eqs. (19) and (20), the relationship of  $q_w$  and  $\Delta T_{\text{sat}}$  is significantly affected by the liquid superheating and may be expressed as  $q_w \propto (\Delta T_{\text{sat}})^n$ , with  $n = 1/2$  for highly subcooled liquid, and  $n = 3/4$  for saturated liquid. Eq. (20) may be rewritten as a dimensionless form

$$Nu = q_w d / (\Delta T_{\text{sat}} \lambda_l) \approx \sqrt{2} Re_1^{1/2} Pr_1^{1/6} ((\lambda_v / \lambda_l) (\Delta T_{\text{sub}} / \Delta T_{\text{sat}}))^{1/2}. \quad (22)$$

### 3. Experimental study

Experiments were conducted on unsteady jet cooling to obtain the boiling heat transfer characteristics. Fig. 2 shows the schematic diagram of the experimental apparatus and Fig. 3 shows the size of the test specimen which is a thin stainless steel (SUS316) flat plate of  $12 \times 12 \text{ mm}^2$  cross-section and 2 mm thickness. A thermocouple was weld at the center of the bottom surface of the specimen and it was linked to a digital high-velocity data recorder to record the temperature response of the specimen. The specimen was preheated to about  $1000^\circ\text{C}$  by a direct current supply device (silicon rectifier), and then stopped heating and removed simultaneously the shutter over the specimen, so that cooling water flowed out from the jet nozzle and impinging on the surface of the specimen. The recorded data for each cooling test were fed to a personal computer and corresponding boiling heat transfer curve was drawn out according to one-dimensional thermal conductive equation

$$c_p \rho \left( \frac{\partial T}{\partial t} \right) = \frac{\partial}{\partial y} \left( \lambda \frac{\partial T}{\partial y} \right). \quad (23)$$

Here,  $c_p \rho = 3935(1 + 0.0004246T) \text{ kJm}^{-3} \text{ K}^{-1}$ ,  $\lambda = 13.47(1 + 0.001163T) \text{ W m}^{-1} \text{ K}^{-1}$ .

In a very small sampling time interval,  $\Delta t$ , between the removed heat quantity inside the specimen and the heat fluxes of the two surfaces of the specimen, there exists following relationship of energy conservation

$$\Delta y \Sigma (\Delta T_i c_p \rho) = (q_w + q_r) \Delta t, \quad (24)$$

where  $\Delta T_i$  denotes the temperature changing at each grid in the time interval,  $\Delta t$ ;  $\Delta y$  denotes the length of grid; and  $q_r$  and  $q_w$  denote the heat flux on the bottom surface and the water cooling surface, respectively. After changing curve of temperature of the bottom surface, namely cooling curve, is obtained experimentally, the radiative heat flux of the bottom surface can be calculated directly (emissivity was taken as a constant of 0.8). The temperature and the heat flux on the water cooling surface can be numerically solved according to Eqs. (23) and (24). In this study, the grid number was

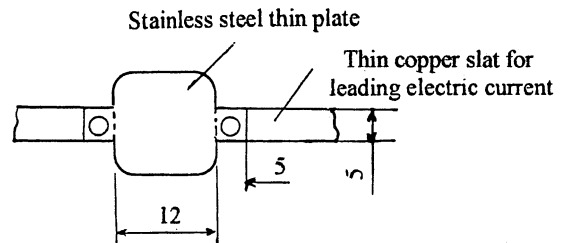


Fig. 3. The size of test specimen.

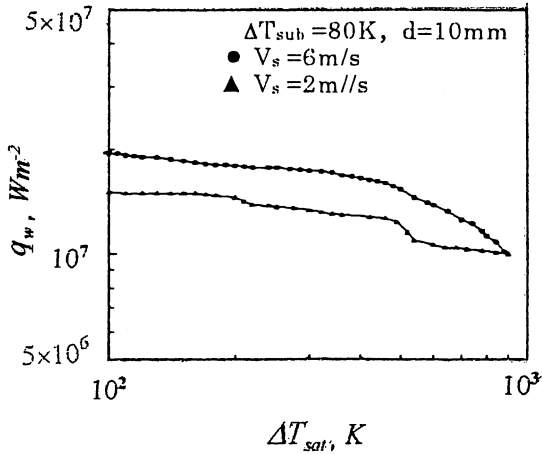


Fig. 4. Experimental results of boiling heat transfer for highly subcooled water.

fixed as 20 ( $\Delta y = 10^{-4}$  m) and the sampling time interval of the digital data recorder was fixed at  $10^{-3}$  s. By trial calculations, the relatively calculating error between both grid numbers of 20 and 40 was less than 1%.

In this experiment, the diameter of jet nozzle was fixed at 10 mm, the impinging velocity ranged from 1 to 3 m s<sup>-1</sup>, and the liquid subcooling ranged from 5 to 80 K. The wave of the impinging velocity was less than  $\pm 4\%$  and the wave of the liquid subcooling was less than

$\pm 0.1$  K. By trial numerical calculations, the heat losses of radiation and thermal conduction from the two sides of the specimen no nearly effect the temperature and the heat flux at the center of the specimen.

4. Results and discussion

Fig. 4 shows the experimental curves of boiling heat transfer for jet impinging of water with a high subcooling,  $\Delta T_{sub} = 80$  K. The heat transfer curves show the characteristics of transition boiling and have not come into film boiling region over whole range of the superheating less than 900 K. Very thin unsteady vapor layer forms actually,  $\delta_v$  is only equal to 3–5  $\mu\text{m}$  by trial calculations, so that the fresh liquid may touch partially with high temperature wall, and hence, transition boiling status occurs.

Fig. 5 shows the predicted values compared to our experimental data on boiling curves of the wall heat flux vs the wall superheating. The impinging velocity and the subcooling of water as fixed reference parameters, respectively. The solid lines are calculated values of Eq. (20) for the liquid subcooling higher than 15 K, and the break line is the calculated values of Eqs. (11)–(16) for low liquid subcooling of 5 and 15 K. The curves with signals are the experimental boiling curves. On the whole, the experimental data are qualitatively coincident with the calculated values and the relations among

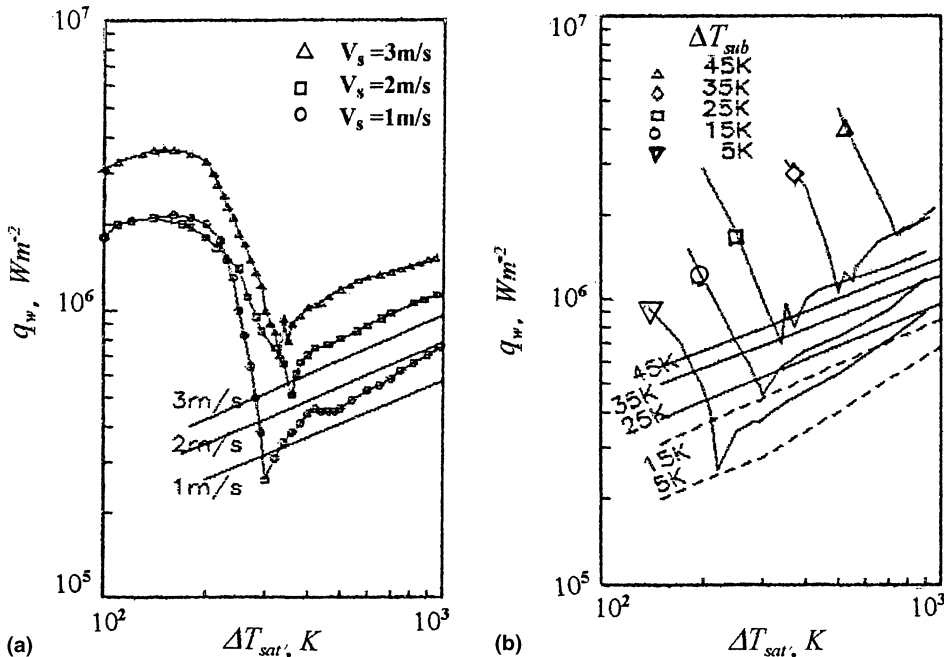


Fig. 5. Comparisons between the predicted values and our experimental data for the stagnation zone with  $d = 10$  mm: (a) for subcooling,  $\Delta T_{sub} = 25$  K; (b) for impinging velocity,  $V_s = 3$  m s<sup>-1</sup>.

parameters are basically right. For low liquid subcooling, the experimental data agree relatively well with the calculated values and are slightly larger than the calculated values. However, for high liquid subcooling, the experimental results are significantly larger than the calculated values. The subcooling has a strong effect on deviation of the experimental data. The subcooling is larger: the vapor layer is thinner, and hence the deviation is greater. This is due to the effect of wavy vapor layer on the heat transfer being stronger with thinner vapor layer.

It is obvious that the wall superheating corresponding to the incipient film boiling point has a strongly foundational relationship with  $\Delta T_{sub}$ , but only a weakly foundational relationship with  $V_s$ . The problem of how to resolve the wall superheating or the minimum heat flux corresponding to the incipient film boiling point relates to the limiting problems of thermodynamics and hydrodynamics, in this paper this problem is not discussed.

Fig. 6 shows the comparisons between predicted values from our proposed model and the experimental data presented by Ishitani et al. [11] on boiling curves of the wall flux vs the wall superheating. The experiment of Ishitani et al. was also a unsteady cooling experiment, but it was a two-dimensional water jet impinging on a flat stainless steel plate of  $12 \times 80 \text{ mm}^2$  cross-section and 2 mm thickness. The width and length of the nozzle were 6.2 and 50 mm, respectively. The experimental data

in film boiling region agree qualitatively well with our predicted values also, the deviation being the same as shown in Fig. 5.

The deviation increases gradually with increasing the liquid subcooling. The reason is mainly due to the effect of waviness of the vapor layer being neglected in our simplified theoretical analysis. This default may be modified by using empirical correlation factor as to be affected by the subcooling and the impinging velocity. If theoretical values of the wall heat flux solved by Eq. (20) are modified by a constant of  $\sqrt{2}$ , such that Eq. (20) is modified as

$$Nu = q_w d / (\Delta T_{sat} \lambda_l) \approx 2Re_1^{1/2} Pr_1^{1/6} ((\lambda_v / \lambda_l) (\Delta T_{sub} / \Delta T_{sat}))^{1/2}, \quad (25)$$

the deviation would be thereby improved as being limited in the range about  $-5\%$  to  $25\%$ .

### 5. Conclusions

1. A simplified model was adopted for predicting the heat transfer characteristics of film boiling of water jet impinging on flat plate at the stagnation zone. Experiments were conducted for comparisons.
2. The water subcooling,  $\Delta T_{sub}$ , provides strong effect on the heat transfer characteristics. The transition boiling occurs for highly subcooled water jet impinging. The

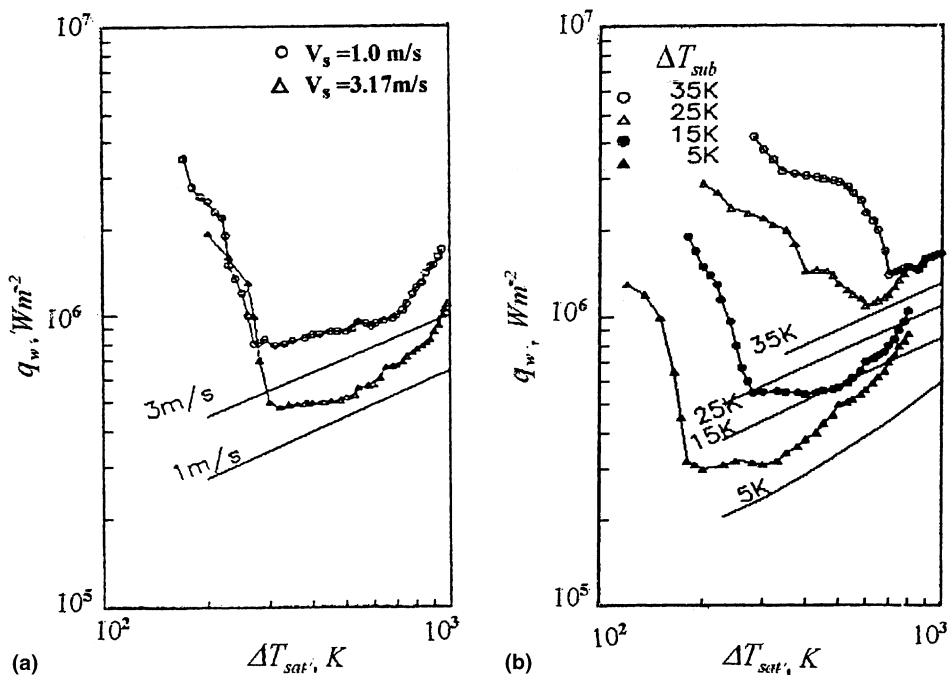


Fig. 6. Comparisons between the predicted values and the experimental data [11] for the stagnation zone with  $d = 6 \text{ mm}$ : (a) for subcooling,  $\Delta T_{sub} = 15 \text{ K}$ ; (b) for impinging velocity,  $V_s = 2.1 \text{ m s}^{-1}$ .

film boiling occurs for lowly subcooled water jet impinging. The wall heat flux increases with the square root of the subcooling.

3. The relationship of  $q_w \propto (V_s/d)^{1/2}$  is available for whole film boiling region.
4. The relationship of  $q_w$  and  $\Delta T_{\text{sat}}$  is significantly affected by the water subcooling, it may be expressed as  $q_w \propto (\Delta T_{\text{sat}})^n$  in general, with  $n = 1/2$  for high water subcooling, and  $n = 3/4$  for the saturated case.
5. The water subcooling could have a strong effect on the incipient film boiling point, while the impinging velocity,  $V_s$ , affects weakly only.
6. Further work would be still needed to check or improve the application of suggested correlating Eq. (25).

## References

- [1] M. Lamvik, B.A. Iden, Heat transfer coefficient by water jets impinging on a hot surface, in: Seventh International Heat Transfer Conference, Munich, FRG, 1982, pp. 369–375.
- [2] H.K. Natsuo, J.I. Okada, H. Takuda, Predictable modeling for cooling process of hot steel plate by a laminar water bar, *Umformtechnik* 55 (4) (1984) 143–148.
- [3] E.M. Sparrow, Analysis of flow field and impinging heat/mass transfer due to a nonuniform slot jet, 1975, ASME J. Heat Transfer (1975) 191–197.
- [4] K. Kunioka, K. Hirata, S. Sugiyama, Study on impinging water cooling of hot plate, *Bull. JASM Ser. B* 45 (390) (1979) 279–285.
- [5] M.C. Han, S. Yoo, G. Yang, J.S. Lee, D.R. Son, Measurements of impinging jet and heat transfer on a semi-circular concave surface, *Int. J. Heat Mass Transfer* 43 (10) (2000) 1811–1822.
- [6] H. Miyazaki, E. Siberman, Flow and heat transfer on a flat plate with a two-dimensional laminar jet issuing from a nozzle of finite height, *Int. J. Heat Mass Transfer* 15 (1972) 2097–2107.
- [7] E.J. Watson, The radial spread of a liquid jet over a horizontal plate, *J. Fluid Mech.* 20 (3) (1964) 481–489.
- [8] D.T. Vader, F.P. Incropera, R. Viskanta, An experimental study of cooling characteristics for water jet impinging a strip mill, *Exp. Thermal Fluid Sci.* 4 (1) (1991) 1–5.
- [9] D.T. Vader, F.P. Incropera, R. Viskanta, Convective nucleate boiling on a heated surface cooling by an impinging planar jet of water, *ASME J. Heat Transfer* 114 (1992) 152–157.
- [10] S. Kumagai, T. Sano, T. Kamata, S. Suzuki, R. Kubo, Boiling heat transfer to an impinging jet in cooling a hot metal slab, *Bull. JASM Ser. B* 60 (570) (1994) 259–263.
- [11] S.K. Ishitani, J.K. Nakanishi, T.A. Hikoshichi, The study of water jet cooling on high temperature plate, in: Proceedings of 13th Japanese National Heat Transfer Conference, 1976-5, Osaka, pp. 343–345.
- [12] D.A. Zumbrennen, R. Viskanta, F.P. Incropera, The effect of surface motion on forced convective film boiling heat transfer, *ASME J. Heat Transfer* 111 (1989) 760–766.
- [13] J. Zhe, H. Sun, C.F. Ma, D. Lei, C. He, Y. Tian, Experimental study on heat transfer of water jet and spraying cooling high temperature wall, *Chinese J. Eng. Thermophysics* 18 (5) (1997) 629–633.
- [14] L.A. Bromley, N.R. Leroy, J.A. Robbers, Heat transfer in forced convection film boiling, *Int. Eng. Chem.* 45 (1) (1953) 2639–2646.